HTML ABSTRACT + LINKS

Influence of vignetting on signal analysis of photocarrier radiometry of semiconductor wafers

Bincheng Li[a)]
Institute of Optics and Electronics, Chinese Academy of Sciences, P. O. Box 350, Shuangliu, Chengdu 610209 People's Republic of China and Center for Advanced Diffusion-Wave Technologies (CADIFT), Department of Mechanical and Industrial Engineering, University of Toronto, Toronto, Ontario, M5S 3G8, Canada

Derrick Shaughnessy and Andreas Mandelis
Center for Advanced Diffusion-Wave Technologies (CADIFT), Department of Mechanical and Industrial Engineering, University of Toronto, Toronto, Ontario, M5S 3G8, Canada

(Received 15 November 2004; accepted 28 March 2005; published online 20 May 2005)

The influence of vignetting on the photocarrier radiometry (PCR) measurements of semiconductor wafers has been investigated both theoretically and experimentally by analyzing the vignetting effect on the PCR amplitude and on the frequency dependence of the PCR amplitude and phase. The vignetting effect significantly reduces the PCR amplitude and modifies the frequency dependencies that are widely used to extract simultaneously the electronic transport properties (that is, the carrier lifetime, the carrier diffusion coefficient, and the front and rear surface recombination velocities) of semiconductor wafers. When using the frequency dependence of the PCR signal to determine the transport properties, the effect of vignetting can be accounted for by an "effective detector size"—a reduced detector size determined by the actual detector size and the vignetting effect. © *2005 American Institute of Physics.* [DOI: 10.1063/1.1921450]

I. INTRODUCTION

In recent years, photothermal radiometry (PTR)[1–7] and photocarrier radiometry (PCR)[8–10] techniques have been extensively used in semiconductor characterization. Both techniques rely on the detection of infrared (IR) emission from the semiconductor sample optically excited by an intensity-modulated laser beam with photon energy greater than the fundamental energy gap of the material. The frequency dependencies of the PTR or PCR amplitude and phase are widely employed to extract the electronic transport properties of semiconductor materials (i.e., minority carrier lifetime τ and diffusion coefficient D, as well as front and rear surface recombination velocities s_1 and s_2).[5–7,9,10] In a typical PTR or PCR experiment, an optical imaging system consisting of a couple of off-axis paraboloidal reflectors[6,8] or (reflective) objectives[7,10] is used to collect, collimate, and focus the IR emission onto an infrared detector, that is, to image the IR emission source onto the detector (usually a liquid-nitrogen-cooled HgCdTe detector or an InGaAs photodiode). The amplitude and phase of the detected PTR or PCR signal depend on the IR emission intensity and profile (determined by the intensity, size, and profile of the excitation beam and by the electronic transport and/or thermal properties of the sample), the collection capacity of the imaging system (determined by the effective sizes and focal lengths of the two objectives, and the distance between them), and the quantum efficiency, size, and shape of the detector. A vignetting effect, which occurs in the IR imaging system, affects the frequency dependencies of both amplitude and phase and therefore has to be appropriately accounted for in data processing in order to correctly extract the transport properties.

In a typical optical imaging system, vignetting occurs for off-axis points where the relative illumination decreases as the radial distance from the optical axis increases. Up to now, little attention has been paid to the vignetting effect of the IR collection systems used in PTR and PCR experiments. Bisson and Fournier[11,12] and Paoloni and Fournier[13,14] reported the effect of diffraction on the thermal diffusivity measurement with PTR microscopy. There has been no report on the vignetting effect in the PTR or PCR systems. The vignetting effect, if not appropriately accounted for, will significantly affect the performance of the PTR or PCR system and the accuracy of the simultaneous determination of the electronic transport and/or thermal parameters of the measured materials. In this article, we report on a detailed investigation of the effect of vignetting on PCR signals and on the determination of the electronic transport properties of semiconductor wafers.

II. EXPERIMENTAL DETAILS

The experimental PCR setup is schematically shown in Fig. 1. A frequency-doubled Nd: yttrium—aluminum–garnet laser (Coherent, CA) pumped tunable Ti: sapphire laser (Coherent, CA) was used as the excitation source. The laser was operated at 830 nm wavelength and the power of the beam was approximately 23 mW. The laser beam was modulated with an acoustic-optic modulator and then focused onto the surface of the sample with a focusing lens. The radius of the beam at the surface was measured by a 5 μm-pinhole scanning and was found to be approximately

[a)]Author to whom correspondence should be addressed; electronic mail: bcli@ioe.ac.cn

 © 2005 American Institute of Physics

Downloaded 18 Jul 2008 to 128.100.49.17. Redistribution subject to AIP license or copyright; see http://rsi.aip.org/rsi/copyright.jsp

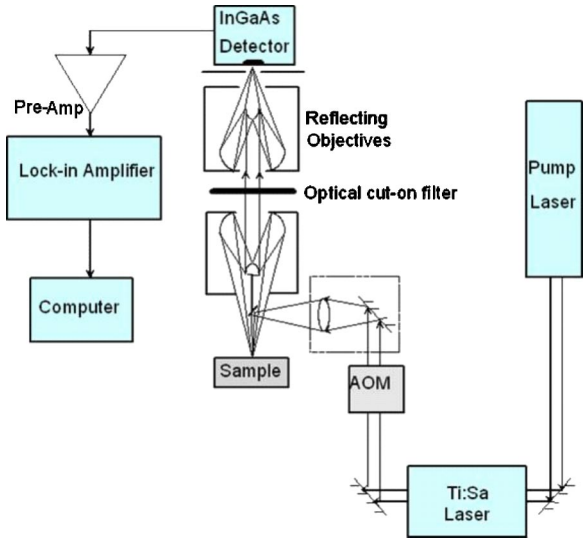

FIG. 1. (Color online). Schematic diagram of PCR experimental setup.

25 μm. The IR emission from the sample was collected and focused onto an InGaAs detector (Thorlabs, NJ) through a pair of reflective objectives (Coherent, CA).[15] The first objective with a numerical aperture (NA) of 0.5 and focal length of 5.41 mm was used to collect and collimate the IR emission, and the second objective with a NA of 0.28 and focal length of 13.35 mm was used to focus the collected IR emission onto the InGaAs detector. The distance between the two objectives was approximately 120 mm. The size of the detector was 1.0 mm in diameter and its spectral response range was 0.8–1.8 μm. A spectrally matched filter was used to further block any leakage of the excitation source. The sample used in this experiment was a (100) oriented nonimplanted *p*-type silicon wafer. The thickness of the sample was approximately 675 μm.

Assuming perfect alignment, in the object field, the relative illumination function of the IR collection optics consisting of two reflective objectives, as used in the PCR setup shown in Fig. 1, was calculated with Zemax®[16] and is presented in Fig. 2 with the dashed line. The difference from the illumination function (the solid line) of a typical two-refractive lens system (with the identical NAs and focal lengths as the two reflective objectives) is due to the effect of the central obscuration of the reflective objectives. The first and second objectives have percentage obscuration of 12.2% and 18.9%, respectively. The optical magnification of the system was 2.47, determined by the ratio of the focal lengths of the second objective to the first one. Due to the vignetting effect, IR emissions outside a circle with a radius of approximately 0.16 mm could not be collected by the detector at the image field.

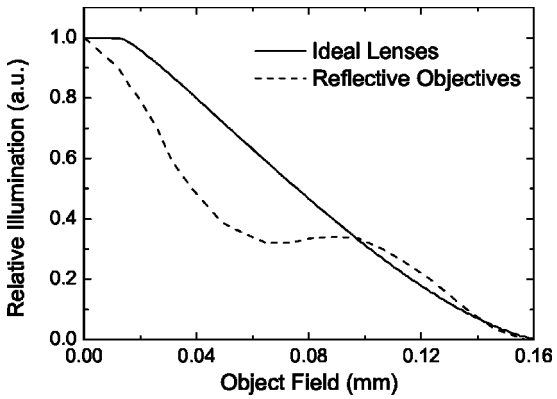

FIG. 2. Relative illumination functions for IR emission collection optics consisting of two refractive lenses (solid line) and two reflective objectives with central obscurations (dashed line).

III. INFLUENCE OF VIGNETTING ON PCR SIGNAL

Since the throughput of the collecting optical system is a function of the radial position at the object field, the collection efficiency of the optical system for IR emission varies with the field coordinate and must be included in the expression for PCR signal. Taking the relative illumination function $H(r)$ into account, the PCR signal measured by a detector with an effective radius a projected into the object field is given as

$$S_{\mathrm{PCR}}(\omega) = 2\pi \cdot \int_0^a S_{\mathrm{PCR\text{-}O}}(r,\omega) H(r) r dr. \tag{1}$$

Where a is the radius of the detector divided by the optical magnification of the two-component collection system. $S_{\mathrm{PCR\text{-}O}}(r,\omega)$ is the IR emission intensity at position r of the object field, which is expressed as follows:[6,8,10]

$$S_{\mathrm{PCR\text{-}O}}(r,\omega) = C \int_0^\infty F(\delta,\omega) J_0(\delta r)\, \delta d\delta \tag{2}$$

with

$$F(\delta,\omega) = \frac{1-\exp(-\beta L)}{\beta}[A + B\exp(\beta L)] + \frac{E}{\alpha}[1-\exp(-\alpha L)], \tag{3}$$

where

$$\beta^2 = \delta^2 + \frac{1+i\omega\tau}{D\tau}, \tag{4}$$

$$E = \frac{\alpha(1-R)\eta P}{2\pi h\upsilon D} \cdot \frac{\exp(-\delta^2 a^2/4)}{\beta^2 - \alpha^2}, \tag{5}$$

$$A = -\frac{1}{H}[a_2 b_1 \exp(\beta L) - a_1 b_2 \exp(-\alpha L)]E, \tag{6}$$

$$B = -\frac{1}{H}[b_1 \exp(-\beta L) - b_2 \exp(-\alpha L)]E, \tag{7}$$

$$H = a_2 \exp(\beta L) - a_1 \exp(-\beta L), \tag{8}$$

$$a_1 = \frac{D\beta - s_1}{D\beta + s_1}, \tag{9}$$

$$b_1 = \frac{D\alpha + s_1}{D\beta + s_1}, \tag{10}$$

Downloaded 18 Jul 2008 to 128.100.49.17. Redistribution subject to AIP license or copyright; see http://rsi.aip.org/rsi/copyright.jsp

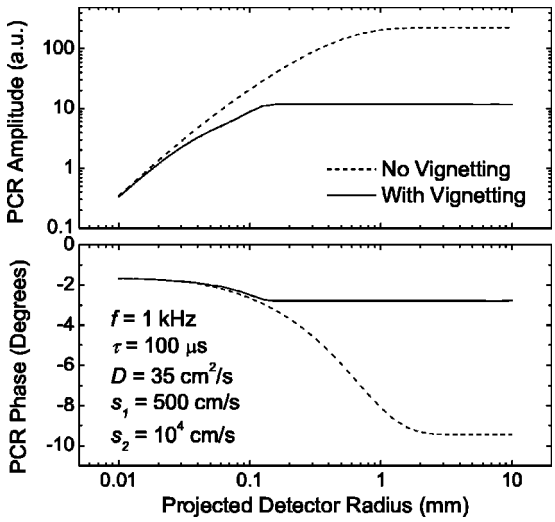

FIG. 3. Calculated PCR amplitude and phase vs the projected detector radius with absence (dashed line) and presence (solid line) of vignetting effect. The assumed parameter values are listed inside the figure. The modulation frequency is assumed to be 1 kHz.

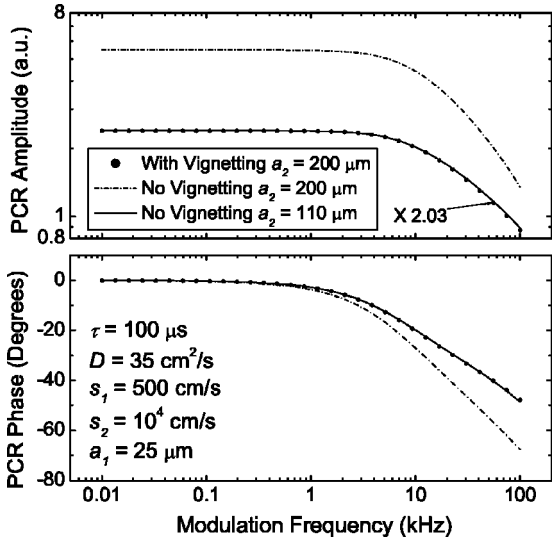

FIG. 4. Theoretical frequency dependencies of PCR amplitude and phase with absence and presence of vignetting effect. The solid points represent the dependencies with the presence of vignetting and a projected detector radius of 200 μm. The amplitude is amplified by a factor of 2.03. The solid and dashed lines represent the dependencies without the presence of vignetting and with a projected detector radius of 200 and 110 μm, respectively.

$$a_2 = \frac{D\beta + s_2}{D\beta - s_2}, \tag{11}$$

$$b_2 = \frac{D\alpha - s_2}{D\beta - s_2}. \tag{12}$$

Here D and τ are the minority carrier diffusion coefficient and lifetime of the sample, and α and L are its absorption coefficient and thickness, respectively; s_1 and s_2 are the front and rear surface recombination velocities of the sample, respectively. R is the reflectivity of the front surface at the excitation wavelength. P and hv are the power and the photon energy of the incident laser beam, $\omega = 2\pi f$ is the angular modulation frequency of the incident laser power and η is the quantum yield, which is the optical-to-electrical energy conversion efficiency. In the following, the influence of the vignetting effect on the PCR signal and on the frequency dependence of the PCR signal are calculated and discussed in detail. The relative illumination function calculated with Zemax® and presented by the dashed line in Fig. 2 is used in the calculations.

To investigate the effect of vignetting on the PCR performance, we first compare the calculated dependencies of PCR amplitude and phase on the projected detector size (that is, the actual detector size divided by the magnification factor of the two-objective system) for cases with the vignetting effect present and absent. The results are presented in Fig. 3. The following electronic transport parameter values of the sample were used in the calculations: $\tau = 0.1$ ms, $D = 35$ cm^2/s, $s_1 = 500$ cm/s, and $s_2 = 10^4$ cm/s. These values are typical for a nonimplanted silicon wafer.[10] The absorption coefficient is assumed to be 6.6×10^4 m^{-1}, which is the absorption coefficient of crystalline silicon (c-Si) at 830 nm wavelength.[17] Without the effect of vignetting, the PCR amplitude first increases rapidly as the detector size increases, and gradually becomes saturated as the influence of the transverse carrier diffusion on the detected PCR signal decreases and eventually becomes negligible. On the other hand, the effect of vignetting is negligible when the detector size is much smaller than the cutoff radius as a smaller detector collects IR emissions only near the center of the IR emission source where vignetting is nearly nonobservable. The influence of vignetting increases as the detector size increases, which results in decreasing PCR amplitude and phase lag. The PCR amplitude becomes independent of the detector size once the projected detector radius becomes larger than the cutoff radius (approximately 0.16 mm). In this case the detected signal is determined solely by the cutoff radius. At low frequency, such that the ac carrier diffusion length is substantially larger than the cutoff radius, vignetting effect reduces the saturated PCR amplitude level to approximately 5% of the saturated value when the vignetting is absent. This is due to the fact that the vignetting effect greatly reduces the contribution of IR emissions at the off-axis points in the object field to the detected PCR signal. For applications requiring high signal-to-noise ratios, such as ion implant dose monitoring,[18] the PCR amplitude level could be increased by over one order of magnitude by redesigning the optical collection system to minimize the vignetting effect.

Since the frequency dependence of the PCR signal is widely used in the simultaneous determination of electronic transport properties (that is, the carrier lifetime τ, the carrier diffusion coefficient D, and the front and rear surface recombination velocities s_1 and s_2) of semiconductor materials via a multi-parameter fitting process, the effect of vignetting on the frequency dependence of the PCR signal directly affects the uniqueness and accuracy of the determined multi-parameter values, and therefore warrants thorough investigation. Frequency scan curves with and without taking into account the vignetting effect are presented in Fig. 4. The projected detector radius at the object field was assumed to be 0.2 mm (the actual detector size divided by the magnification factor). The frequency behavior with and without the

Downloaded 18 Jul 2008 to 128.100.49.17. Redistribution subject to AIP license or copyright; see http://rsi.aip.org/rsi/copyright.jsp

vignetting effect is quite different. This is because the contribution of IR emissions at the off-axis points to the detected PCR signal is frequency dependent, and both the frequency dependence and the vignetting effect have a different radial dependence. The off-axis contribution decreases with the increasing frequency as the photocarriers are confined more locally to the excitation source as the frequency increases. They are located at the center of the object field, where the vignetting effect is minimal. The influence of the vignetting effect on the PCR amplitude and phase therefore decreases with increasing frequency, a fact which results in pronounced differences between the signal frequency dependencies in the absence and presence of the vignetting effect. However, if only the self-normalized PCR amplitude is considered, the PCR frequency scan in the presence of vignetting effect can be fitted with a reasonable accuracy using a theoretical model that does not account for the presence of vignetting effect but with a reduced detector size, as presented in Fig. 4. We refer to the reduced detector radius as "effective detector radius." For the example presented in Fig. 4, the effective detector radius is approximately 110 μm, compared to the actual projected detector radius of 200 μm.

Since a complete PCR theoretical model which takes into account the vignetting effect is too complicated (it requires a double integration) to be used in a multi-parameter fitting procedure to simultaneously extract the transport properties of the investigated sample, the PCR model without accounting for the vignetting effect has to be used in the multi-parameter fitting. The use of the effective detector radius could significantly simplify the multi-parameter fitting process for the measurement of the electronic transport properties by avoiding the use of the complicated theoretical model. However, care has to be taken when determining the effective detector size, as simulation results show the value of the fitted effective detector radius depends slightly on the transport properties of the reference sample. For example, assuming a lifetime of 0.1 ms, a minority electron diffusion coefficient in *p*-type material of 35 cm^2/s, and a front surface recombination velocity of 500 cm/s, the best-fitted effective detector radius is 110 μm. The effective detector radius changes to 105 μm if the diffusion coefficient is that of minority holes in *n*-type material (12 cm^2/s). If the lifetime is 5 μs and the front surface recombination velocity is 1×10^5 cm/s, the effective detector size then reduces to 100 μm. Therefore, for optimal measurement accuracy the reference sample used to determine the effective detector size should have transport properties very close to those of the investigated samples. It is worth mentioning that once the projected detector size is larger than the cutoff size determined by the vignetting effect, the effective detector size is solely determined by the vignetting effect and the transport properties of the reference sample, independent of the actual size of the detector.

IV. EXPERIMENTAL RESULTS AND DISCUSSIONS

Experimentally the vignetting effect was investigated by measuring the radial position dependence of the PCR amplitude while scanning a 50 μm pinhole and an InGaAs detector assembly across the detection field. Considering the optical magnification of the IR collection system, the spatial resolution of the detector was approximately 20 μm at the object field. Figure 5 shows the theoretical and experimental amplitudes of the PCR signal as a function of radial position at the object field for a nonimplanted silicon wafer, with and without the presence of the vignetting effect. The full circles represent experimental results. The solid line is the theoretical result considering the vignetting effect and the dashed line is theoretical results without accounting for the vignetting. The assumed values of parameters were $\tau=70$ μs, $D=35$ cm^2/s, $s_1=412$ cm/s, and $s_2=10^4$ cm/s, respectively. When the effect of vignetting was taken into account, good agreement between theory and experiment was obtained around the central region. The signal was cut off at approximately 0.16 mm from the central position, in agreement with the theoretical prediction. The difference near the edge may be due to possible misalignment of the system, and the depth distribution and multi-reflections of the IR emissions inside the sample that are not considered in the theoretical model. It should be mentioned that perfect alignment of the whole PCR system, especially the IR collection optics, is extremely difficult, as the photocarrier IR emissions are invisible and extremely weak. Experimentally, the system is aligned to maximize the PCR signal amplitude by iteratively adjusting the longitudinal positions of the sample and the detector and the lateral (transverse and horizontal) positions of the two reflective objectives. Care was taken to avoid double peaks of the PCR signal at the detection plane. The presence of double peaks was an indication that the two objectives were certainly misaligned, though the absence of the double peaks did not necessarily imply a perfect alignment of the two objectives.

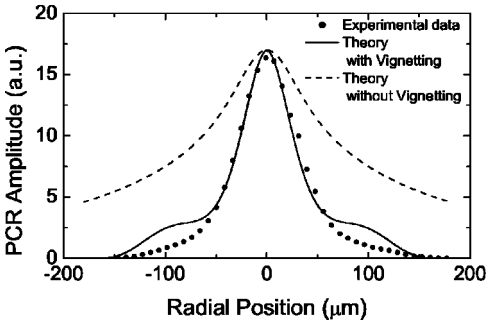

FIG. 5. Theoretical (solid and dashed lines) and experimental (solid points) PCR amplitudes vs the radial position at the object field. The modulation frequency was 1 kHz. The solid and dashed curves represent the calculated PCR amplitudes as function of the radial position with the presence and absence of the vignetting effect.

The frequency dependence of the PCR signal for a nonimplanted *p*-type silicon wafer was then measured and the results are presented in Fig. 6. The frequency dependence was recorded with two lock-in amplifiers (LIAs). The first LIA (SRS Model SR850) recorded the PCR signal from 100 Hz to 100 kHz and the second one (SRS Model SR844) recorded the signal from 100 kHz to 1 MHz. Together the amplitude and phase of the PCR signal were recorded at a total of 32 frequency points spanning from 100 Hz to 1 MHz. To eliminate the influence of the instrumental transfer

Downloaded 18 Jul 2008 to 128.100.49.17. Redistribution subject to AIP license or copyright; see http://rsi.aip.org/rsi/copyright.jsp

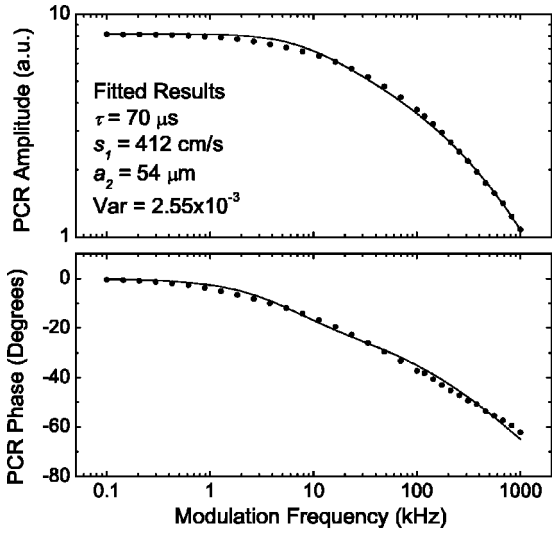

FIG. 6. Experimental frequency dependencies of the PCR amplitude and phase (solid points) and the corresponding best fits (solid lines) to the theoretical model without considering the vignetting effect, for a nonimplanted silicon wafer. The best fits result in an optimal detector radius of 54 μm, which is much smaller than the projected detector radius, 200 μm, due to the influence of vignetting effect and system misalignment.

function, the amplitude and phase of the PCR signal were normalized by the detector signal recorded with the scattered light of the excitation beam (in this case the filter in front of the detector was removed). After normalization, the amplitudes and phases recorded with the two LIAs were merged in the overlapping frequency range (around 100 kHz). The measured frequency dependencies of the PCR amplitude and phase were then fitted to the theoretical model[6,10] without the presence of the vignetting effect via a least-squares process to determine an effective detector radius. The effective detector radius was later used as a known parameter in multiparameter fittings for determining the electronic transport properties of ion-implanted silicon wafers.[19] In the fitting, the lifetime and front surface recombination velocity of the sample, as well as the effective detector radius, were set as free parameters to minimize the following mean square variance:

$$Var = \frac{\sum_{i=1}^{N}\left(1-\frac{A_T(f_i)}{A_E(f_i)}\right)^2}{N} + \frac{\sum_{i=1}^{N}[\phi_T(f_i)-\phi_E(f_i)]^2}{\sum_{i=1}^{N}[\phi_E(f_i)]^2}. \quad (13)$$

Here $A_T(f_i)$ and $A_E(f_i)$, and $\phi_T(f_i)$ and $\phi_E(f_i)$ are the theoretical and experimental PCR amplitudes and phases at modulation frequency f_i, respectively. N is the total number of data points. The carrier diffusion coefficient and rear surface recombination velocity were assumed to be 35 and 10^4 cm/s, respectively. The accurate value of the rear surface recombination velocity is not critical, as for this sample the PCR signal has a low sensitivity to back surface recombination in the used frequency range.[20] The fitted lifetime and front surface recombination velocity were 70 μs and 412 cm/s, respectively, in agreement with typical values for nonimplanted silicon wafers. The fitted effective detector radius was approximately 54 μm, much smaller than the estimated theoretical value, 103 μm, assuming a perfect alignment of the IR collection optics. This discrepancy is believed to be due mainly to (1) misalignment of the PCR system as mentioned above; (2) the multi-reflections of IR emissions at the front and rear surfaces; and (3) the depth distribution of the IR emissions inside the sample. Both (2) and (3) cause image blurring at the detection plane, result in defocusing of the IR emission source at the detector surface and therefore a reduction of the fitted effective detector size. The good agreement between the experimental frequency scan and the theoretical fit indicated that, for determining the electronic transport properties of semiconductor wafers via frequency scan and multi-parameter fitting, the influence of vignetting occurred in the IR collection optics and even misalignment of the system can be properly accounted for by a reduced effective detector radius.

Theoretical and experimental results have shown that the vignetting effect significantly affects the PCR amplitude measurement and frequency scans, and therefore has to be properly addressed, in order to extend the applications of the PCR technique to quantitative implantation dose monitoring, electronic transport characterization of semiconductor materials, etc. Even though the vignetting effect has been considered only for a specific PCR system employing two reflective objectives to collect the IR emissions, vignetting is a common phenomenon affecting PCR, PTR, and other IR emission based systems in which it is difficult or impossible to collect all diffusely emitted photons and therefore to completely avoid the vignetting effect. A practical PCR or PTR system design should be optimized by compromising the spatial resolution, collection angle, and the vignetting effect. In any PCR or PTR systems where high spatial resolution is critical, the IR emission collection optics used in such systems usually presents strong vignetting effect that has to be properly corrected in data processing. In this case the effective detector radius approach has been shown to be a promising method to cancel the influence of vignetting.

ACKNOWLEDGMENTS

The financial support of Materials and Manufacturing Ontario (MMO) through a Collaborative Contract to A.M. and of the Natural Science and Engineering Council of Canada (NSERC) is gratefully acknowledged. The authors thank Guomao Tang for calculating the relative illumination function.

[1] A. Mandelis, A. Othonos, C. Christofides, and J. Boussey-Said, J. Appl. Phys. **80**, 5332 (1996).
[2] A. Salnick, A. Mandelis, and C. Jean, Appl. Phys. Lett. **69**, 2522 (1996).
[3] A. Salnick, A. Mandelis, H. Ruda, and C. Jean, J. Appl. Phys. **82**, 1853 (1997).
[4] T. Ikari, A. Salnick, and A. Mandelis, J. Appl. Phys. **85**, 7392 (1999).
[5] M. E. Rodríguez, A. Mandelis, G. Pan, J. A. García, V. Gorodokin, and Y. Raskin, J. Appl. Phys. **87**, 8113 (2000).
[6] D. Shaughnessy and A. Mandelis, J. Appl. Phys. **93**, 5236 (2003).
[7] D. Shaughnessy and A. Mandelis, J. Appl. Phys. **93**, 5244 (2003).
[8] A. Mandelis, J. Batista, and D. Shaughnessy, Phys. Rev. B **67**, 205208 (2003).
[9] J. Batista, A. Mandelis, and D. Shaughnessy, Appl. Phys. Lett. **82**, 4077 (2003).
[10] B. Li, D. Shaughnessy, A. Mandelis, J. Batista, and J. Garcia, J. Appl.

Downloaded 18 Jul 2008 to 128.100.49.17. Redistribution subject to AIP license or copyright; see http://rsi.aip.org/rsi/copyright.jsp

Phys. **96**, 186 (2004).
[11] J. F. Bisson and D. Fournier, J. Appl. Phys. **83**, 1036 (1998).
[12] J. F. Bisson and D. Fournier, J. Appl. Phys. **84**, 38 (1998).
[13] S. Paoloni and D. Fournier, J. Appl. Phys. **92**, 5950 (2002).
[14] S. Paoloni and D. Fournier, J. Appl. Phys. **92**, 5955 (2002).
[15] Visit www.ealingcatalog.com for details of the two reflective objectives. The catalog numbers for objectives 1 and 2 are 25-0522 and 25-0506, respectively.
[16] Zemax® is an optical design software developed by the ZEMAX Development Corporation (San Diego, CA). Visit www.zemax.com for details about the product.
[17] *Handbook of Optical Constants of Solids*, edited by E. D. Palik (Academic, San Diego, 1998), Vols. I and III.
[18] D. Shaughnessy, B. Li, A. Mandelis, and J. Batista, Appl. Phys. Lett. **84**, 5219 (2004).
[19] B. Li, D. Shaughnessy, and A. Mandelis, J. Appl. Phys. **96**, 186 (2004).
[20] B. Li, D. Shaughnessy, and A. Mandelis, J. Appl. Phys. **97**, 023701 (2005).

Downloaded 18 Jul 2008 to 128.100.49.17. Redistribution subject to AIP license or copyright; see http://rsi.aip.org/rsi/copyright.jsp